

1 **Supplemental Methods**

2 *Humans*

3 Nine patients with a DSM-IV diagnosis of schizophrenia (7 men, 2 women) were
4 recruited from the Iowa Longitudinal Database and 9 sex-, education- and age-matched controls
5 (7 men, 2 women) recruited from the University of Iowa Department of Neurology’s Cognitive
6 Neuroscience Registry for Normative Data (Table 1 for patient data). Matched controls had no
7 history of significant psychiatric, neurological or medical illnesses. All participants were
8 determined to have the decisional capacity to provide informed consent, resided within 100 miles
9 of Iowa City and were able to independently travel to the University of Iowa Hospitals and
10 Clinics.

11

12 *Human Interval timing task*

13 Interval timing was investigated in humans with and without schizophrenia according to
14 methods described at length previously¹. The interval timing task consisted of 4 blocks of 40
15 trials (160 trials in total). Trials were presented in pseudorandom order. All trials began when a
16 numerical cue stimulus appeared on the center of the screen indicating the temporal interval the
17 participants were instructed to estimate (3 or 12 s – 3 s trials were excluded in this study).
18 Participants made responses by pressing the space bar on a keyboard using their dominant hand
19 when they estimated the temporal interval had elapsed. Participants received feedback about
20 their response time at the end of each trial. There was a 3-6 s interval between response and
21 feedback. After feedback, participants moved to the next trial by pressing the space bar. The task
22 was self-paced and the participants were asked not to count in their head during the task.
23 Participants performed 4 practice trials prior to the real task. The interval-timing task consisted

24 of 160 trials with either a 3 or 12 s interval; only data from the 12 s interval was included in this
25 manuscript. All trials began when a numerical cue stimulus appeared on the center of the screen
26 indicating the temporal interval the participants were instructed to estimate (3 or 12 s).
27 Participants made responses by pressing the space bar on a keyboard using their dominant hand
28 when they estimated the temporal interval had elapsed. Participants received feedback about
29 their response time at the end of each trial. There was a uniformly varying, randomly chosen 3-
30 to 6-s interval between response and feedback. After feedback, participants moved to the next
31 trial by pressing the space bar again. The task was self-paced, and the participants were asked not
32 to count in their head during the task.

33

34 *EEG Recording and analysis*

35 EEG recording and analysis was similar to methods described in detail in prior work^{1,6}.
36 EEG was recorded on a Nihon Kohden system with a sampling rate of 500 Hz. EEG was
37 recorded from 21 channels based on the 10-20 system (Fz, Cz, Pz, FP1/2, F3/4, C3/4, P3/4, F7/8,
38 T3/4, T5/6, O1/2, M1/2), as well as left-eye VEOG and ground (forehead). This approach was
39 selected to match our previous EEG datasets that described differences in low-frequency rhythms
40 between patients with Parkinson's disease and controls^{1,7}. Impedance of all electrodes was below
41 5 k Ω . Continuous data were parsed in to 16 s epochs (-2 to 14 seconds following the cue) and re-
42 referenced to the mathematical average of the two mastoid channels, yielding a total of 19 scalp
43 EEG channels. Eye blinks and horizontal eye movements were removed by hand using
44 independent component analysis and EEGLab⁸. Time-frequency measures were computed by
45 multiplying the fast Fourier transformed (FFT) power spectrum of single trial EEG data with the

46 FFT power spectrum of a set of complex Morlet wavelets (defined as a Gaussian-windowed
47 complex sine wave: $e^{i2\pi t f} e^{-t^2/(2 \times \sigma^2)}$, where t is time, f is frequency (which increased from 1
48 to 50 Hz in 50 logarithmically-spaced steps), and σ defines the width (or “cycles”) of each
49 frequency band, set according to $4/(2\pi f)$), and taking the inverse FFT. The end result of this
50 process is identical to time-domain signal convolution, and it resulted in estimates of
51 instantaneous power (the magnitude of the analytic signal). Each epoch was then cut in length (-
52 0.5 to +2 s). Power was normalized by conversion to a decibel (dB) scale
53 ($10 \times \log_{10}(\text{power}_t / \text{power}_{\text{baseline}})$), allowing a direct comparison of effects across frequency bands.
54 The baseline for each frequency consisted of the average power from -0.5 to -0.3 s prior to the
55 onset of the cues. Human time-frequency plots and ERPs were analyzed from electrode Cz in
56 delta (1- 4 Hz) and theta (5-8 Hz) in accordance with well-established prior hypotheses^{1,4}. Two
57 additional electrodes were placed 1 cm below the inion and 2 cm lateral to record activity from
58 cerebellar hemispheres.

59

60 *Rodents*

61 Animals were motivated by regulated access to water, while food was available *ad*
62 *libitum*. Rats consumed 10-15 mL of water during each behavioral session and additional water
63 (5-10 mL) was provided 1-3 hours after each behavioral session in the home cage. Single
64 housing and a 12 hour light/dark cycle were used; all experiments took place during the light
65 cycle. Rats were maintained at ~90% of their free-access body weight during the course of these
66 experiments and received one day of free access to water per week. All procedures were
67 approved by the Animal Care and Use Committee at the University of Iowa.

68 *Rodent Interval timing task*

69 All rats were trained to perform an interval timing task according to previously published
70 methods^{3-5,9}. Animals learned to make operant lever presses to receive liquid rewards. After
71 fixed-ratio training, animals were trained in a 12 s fixed-interval timing task in which rewards
72 were delivered for responses after a 12 s interval. Rewarded presses were signaled by a click and
73 an ‘off’ house light. Once they were well-trained, a second light was added on the right side of
74 lever to indicate a shorter, 3 s interval (these trials were not included in this study). Each
75 rewarded trial was followed by a 6, 8, 10 or 12 s pseudorandom intertrial interval which
76 concluded with an ‘on’ house light signaling the beginning of the next trial. Early responses
77 occurring before interval end were not reinforced. The house light was turned on at trial onset
78 and lasted until the onset of the intertrial interval, which began when the rewarded press was
79 made or a time-out occurred after 18 seconds on trials with no responses. Training and infusion
80 sessions were 60 minutes long. Mean response time was defined as the average time the animals
81 pressed the lever on each trial, which is used to estimate animals' internal estimates of time⁴. All
82 behavior took place in operant chambers (MedAssociates, St Albans, VT) equipped with a lever,
83 a drinking tube, and a speaker driven to produce an 8 kHz tone at 72 dB. Behavioral arenas were
84 housed in sound-attenuating chambers (MedAssociates). Water rewards were delivered via a
85 pump (MedAssociates) connected to a metal drinking tube (AnCare) via Tygon tubing.

86

87 *Rodent surgery*

88 Rats were trained in the interval timing task, assigned to an experimental group, and
89 implanted accordingly. The MFC and LCN of rats trained in the two interval task were implanted

90 with microwire arrays, 33-gauge infusion cannula (Plastics One), or fiber optics and ChR2
91 according experimental protocol. The coordinates for the left medial frontal implants were AP:
92 +3.2, ML: ± 1.2 , DV: -3.5 @ 12° in the lateral plane; for the left ventrolateral thalamus: AP: -2.3,
93 ML: ± 1.8 , DV: -5.4; and for right lateral cerebellar nuclei AP: -10.8, ML: ± 3.6 , DV: -6.2. A
94 surgical level of anesthesia was maintained with hourly (or as needed) ketamine supplements (10
95 mg/kg). The electrode array was inserted while concurrently recording neuronal activity to verify
96 implantation in layer II/III of the MFC or the LCN. The craniotomy was sealed with
97 cyanoacrylate ('SloZap', Pacer Technologies, Rancho Cucamonga, CA) accelerated by
98 'ZipKicker' (Pacer Technologies), and methyl methacrylate (i.e., dental cement; AM Systems,
99 Port Angeles, WA). Following implantation, animals recovered for one week before being
100 reacclimatized to behavioral and recording procedures.

101

102 *Rodent perfusions*

103 When experiments were complete, rats were anesthetized, sacrificed by injections of 100
104 mg/kg sodium pentobarbital, and transcardially perfused with 10% formalin. Brains were post
105 fixed in a solution of 10% formalin and 20% sucrose before being sectioned on a freezing
106 microtome. Brain slices were mounted on gelatin-subbed slides and stained for cell bodies using
107 DAPI. Histological reconstruction was completed using post mortem analysis of electrode and
108 cannula placements and confocal microscopy in each animal. These data were used to determine
109 electrode, infusion cannula, optical cannula, and spread of viral infection according to each
110 experiment.

111

112 *Focal drug infusions*

113 Focal drug infusions into MFC and LCN were performed according to procedures
114 described previously^{4,5,9}. On subsequent days while anesthetized via isoflurane, the MFC was
115 infused with 0.9% saline (Phoenix Scientific, St. Joseph, MO) during control sessions or D1-
116 dopamine receptor antagonist SCH23390 (0.5 μg of 1.0 $\mu\text{g}/\mu\text{L}$)^{4,10}. Infusions were conducted by
117 inserting an injector into the cannula and 0.5 μL of infusion fluid was delivered at a rate of 30
118 $\mu\text{L}/\text{hr}$ (0.5 $\mu\text{L}/\text{min}$) via a syringe infusion pump (KDS Scientific, Holliston, MA). After the
119 injection was complete, the injector was left in place for 2 minutes to allow for diffusion.
120 Infusions were counterbalanced and always separated by 24 hours.

121

122 *Optogenetic stimulation of the LCN projections to the ventrolateral thalamus*

123 To target the cerebellar output pathways originating in lateral cerebellar nuclei, an AAV
124 viral construct CamKII-ChR2 and CamKII-mCherry was infused in LCN. An optical fiber
125 cannula (200 μm core, 0.22NA, Doric Lenses) was implanted in the ventrolateral thalamus to
126 specifically target terminals expressing ChR2 in the LCN-VL pathway. Rats were injected with
127 AAV-ChR2 into LCN, with immediate placement of an optical fiber cannula (200 μm core,
128 0.22NA, Doric Lenses). The injection consisted of 0.5 microliters of $\sim 10^{11}$ infectious particles
129 per milliliter. A separate group of 6 control animals were injected with AAV- CamKII-mCherry.
130 No randomization or blinding was used to select these animals. During testing, each rat
131 performed the fixed-interval timing task for 1 hr with op togenetic stimulation on half of
132 pseudorandomly chosen trials. In stimulation sessions, 473 nm light was delivered at 10 mW

133 power on 50% of trials. Task performance and neuronal activity was compared between
134 illuminated and unilluminated trials within each animal on the test day.

135

136 *Neurophysiological analyses*

137 Neuronal ensemble recordings in the MFC were acquired using a multi-electrode
138 recording system (Plexon, Dallas, TX). Putative single neurons were identified on-line using an
139 oscilloscope and audio monitor. The Plexon off-line sorter was used to analyze the signals after
140 the experiments and to remove artifacts. Spike activity was analyzed for all cells that fired at
141 rates above 0.1 Hz. Statistical summaries were based on all recorded neurons. Principal
142 component analysis (PCA) and waveform shape were used for spike sorting. Single units were
143 identified as having 1) consistent waveform shape, 2) separable clusters in PCA space, and 3) a
144 consistent refractory period of at least 2 ms in interspike interval histograms. Preliminary
145 analysis of neuronal activity and quantitative analysis of basic firing properties were carried out
146 using NeuroExplorer (Nex Technologies, Littleton, MA), and quantitative analyses were
147 performed with custom routines for MATLAB. Peri-event rasters and average histograms were
148 constructed around light on, lever release, lever press, and lick. Microwire electrode arrays were
149 comprised of 16 electrodes. Local field potential (LFPs) were recorded from 4 of these
150 electrodes per rodent. LFP channels were analog filtered between 0.7 and 100 Hz online and
151 recorded in parallel with single unit channels using a wide-band board. In each animal, one
152 electrode without single units was reserved for local referencing. Recordings from this reference
153 electrode did not have single units and had minimal line noise, and this electrode was used for
154 local referencing for both single unit and LFP recordings.

155 For single-unit recordings, peri-event time histograms were calculated by recording the
156 time of each putative action potential around cue onset with 0.01 s bins. Each occurrence of the
157 cue was considered a trial, and putative action potentials were plotted relative to these events (0-
158 12 s) using a raster plot. Histograms were calculated by taking the average firing rate and
159 smoothing over 1 s using a Gaussian window. Data were tested for normality prior to
160 subsequent analyses.

161 We defined time-related ramping activity as firing rate that progressed uniformly over the
162 interval. We measured this in two ways: PCA and linear regression. PCA was used to identify
163 dominant patterns of neuronal activity using orthogonal basis functions from peri-event
164 histograms during the 12 s interval^{4,5}. All neurons from both areas were included in PCA. The
165 same principal components were projected onto MFC and LCN recordings, and PC weights were
166 compared via a t-test⁴. Secondly, we used regression to define neuronal ramping activity
167 according to the formula:

$$168 \quad y = at+bt^2+c$$

169 Where y is firing rate, t is the time in seconds, and a is the linear slope and b is quadratic slope.
170 Goodness of fit was derived from an ANOVA¹¹.

171 Correlation analysis (MATLAB function PARTIALCORR) was used to explore the
172 relationship of spiking activity average response time and other neurons using Pearson's
173 correlation⁴. Only 12 s trials were used for correlation data. Response time was defined by the
174 average time the animals pressed the lever on each trial and can be used to estimate animals'
175 internal estimate of time⁴. If the animal made multiple presses on a single trial, response times
176 were averaged. In this analysis, response time was treated as a continuous variable. Interval

177 epochs were divided into 3 s windows for correlation; as most movements occurred after 6 s,
178 these epochs were excluded from analyses. Trial-by-trial correlations of firing rate were created
179 by performing partial correlation of firing rate over the entire interval on each trial for two
180 neurons, accounting for heavier correlations with average response time. Joint peristimulus trial
181 histograms were calculated at 0.1 and 1 s bins during the interval, and the shift-predicted matrix
182 was subtracted from the raw matrix. In both cases, shuffled correlations were generated by
183 randomly permuting trial order for comparisons. Analysis of fast interactions was performed by
184 canonical cross-correlation, spike-spike coherence, analysis of neuronal synchrony and by
185 performing the above analysis at smaller bin sizes (1 to 100 ms).

186 Time-frequency calculations were computed using custom-written MATLAB routines
187 using identical approaches to EEG data above^{4,5,9,12}. To examine the time-frequency component
188 of interactions between individual spikes and the field potential, we applied spike-field
189 coherence analysis using the Neurospec toolbox^{4,6,13}, in which multivariate Fourier analysis was
190 used to extract phase-locking among spike trains and local field potentials. Phase-locking
191 coherence values varied from 0 to 1, where 0 indicates no coherence, and 1 indicates perfect
192 coherence. To compare across neurons with different coherence distributions, all phase-locking
193 values were divided by the 95% confidence for each interval, so that 1 indicates a $p < 0.05$.

194 Correlated neurons were selected as those that had Pearson's correlation coefficient summed at
195 > 5 across the entire ensemble. Only neurons with a firing rate > 1 Hz were analyzed for spike-
196 field coherence. All code available from:

197 <http://www.healthcare.uiowa.edu/labs/narayanan/resources.html>

198

200 Nine MFC LFPs and nine LCN LFPs recorded in 3 rodents were downsampled to 200Hz
201 and a 59-61 Hz Butterworth notch filter was applied to remove line noise. We selected a model
202 order of 500ms and 2000ms sliding time segments (6 segments per 12s interval timing trial) for
203 subsequent analysis to maximize the resolution of low frequency Granger prediction. A model
204 order of 500ms contains ≥ 1 cycle of a ≥ 2 Hz oscillation, allowing increased frequency
205 specificity of Granger prediction. Therefore, we subtracted single-subject ERPs from time series
206 segments, detrended and z-scored all modeled data. To visualize bandlimited directed
207 connectivity, *armorf.m* derived autoregression coefficient matrices were Fourier transformed and
208 inverted to generate transfer functions for the spectral factorization of autoregression residuals
209 (Fig 3F)¹⁴. Spectral pairwise Granger prediction was subsequently calculated by inverse Fourier
210 transformation of spectral factorization outputs, resulting in time-frequency domain connectivity
211 estimates¹⁴. Optimal VAR model order was determined by varying model order across repeated
212 bivariate Granger parameter estimates using the BSMART toolbox function *armorf.m*, then
213 inputting residuals matrices into Bayes information criterion (BIC) tests as described
214 previously¹⁴. Mean BIC values across segments converged to a stable minimum across orders $>$
215 100 ms, indicating minimized regression error (Fig S7A). Time series segments were submitted
216 to KPSS unit root testing using MVGC Toolbox routines to determine single trial KPSS test
217 statistics. Statistical testing of stationarity was performed by compared single trial test statistics
218 to a nonstationarity critical value computed at $p = 0.05$ (Fig S7B)¹⁴. Significant Granger
219 causality during 12s interval timing was assessed using Granger's F-test routines in MVGC
220 Toolbox at $p = 0.05$. Inputs were F-statistics grand averaged across animals and time segments
221 for directed connectivity between MFC and LCN in experimental and time-shuffled data.

222

223

224 *Power analysis*

225 The statistical power for each comparison was calculated for each test in using the matlab
226 function `sampsizepwr.m` by assuming a *t* or a *chi-square* distribution where appropriate, and
227 assuming comparisons between two independent samples using two-tailed tests. These power
228 analyses were used to estimate human and animal sample sizes.

229

230

231

232

233

234

235

236

237

238

239

240

241

242

243

244

245

246

247

248

249 **Supplementary References**

250

251 1 Parker KL, Chen K-H, Kingyon JR, Cavanagh JF, Naryanan NS. Medial frontal ~4 Hz
252 activity in humans and rodents is attenuated in PD patients and in rodents with cortical
253 dopamine depletion. *J Neurophysiol* 2015; : jn.00412.2015.

254 2 Fry W, Kelleher RT, Cook L. A mathematical index of performance on fixed-interval
255 schedules of reinforcement. *J Exp Anal Behav* 1960; **3**: 193–199.

256 3 Narayanan NS, Land BB, Solder JE, Deisseroth K, DiLeone RJ. Prefrontal D1 dopamine
257 signaling is required for temporal control. *Proc Natl Acad Sci U S A* 2012; **109**: 20726–
258 20731.

259 4 Parker KL, Chen K-H, Kingyon JR, Cavanagh JF, Narayanan NS. D1-Dependent 4 Hz
260 Oscillations and Ramping Activity in Rodent Medial Frontal Cortex during Interval Timing.
261 *J Neurosci* 2014; **34**: 16774–16783.

262 5 Parker KL, Ruggiero RN, Narayanan NS. Infusion of D1 Dopamine Receptor Agonist into
263 Medial Frontal Cortex Disrupts Neural Correlates of Interval Timing. *Front Behav Neurosci*
264 2015; **9**: 294.

265 6 Narayanan NS, Cavanagh JF, Frank MJ, Laubach M. Common medial frontal mechanisms of
266 adaptive control in humans and rodents. *Nat Neurosci* 2013; **16**: 1888–1897.

267 7 Chen K-H, Okerstrom KL, Kingyon JR, Anderson SW, Cavanagh JF, Narayanan NS. Startle
268 Habituation and Midfrontal Theta Activity in Parkinson’s Disease. *J Cogn Neurosci* 2016; :
269 1–11.

270 8 Delorme A, Makeig S. EEGLAB: an open source toolbox for analysis of single-trial EEG
271 dynamics including independent component analysis. *J Neurosci Methods* 2004; **134**: 9–21.

272 9 Parker KL, Chen K-H, Kingyon JR, Cavanagh JF, Naryanan NS. Medial frontal ~4 Hz
273 activity in humans and rodents is attenuated in PD patients and in rodents with cortical
274 dopamine depletion. *J Neurophysiol* 2015; : jn.00412.2015.

275 10 Parker KL, Alberico SL, Miller AD, Narayanan NS. Prefrontal D1 dopamine signaling is
276 necessary for temporal expectation during reaction time performance. *Neuroscience* 2013.
277 doi:10.1016/j.neuroscience.2013.09.057.

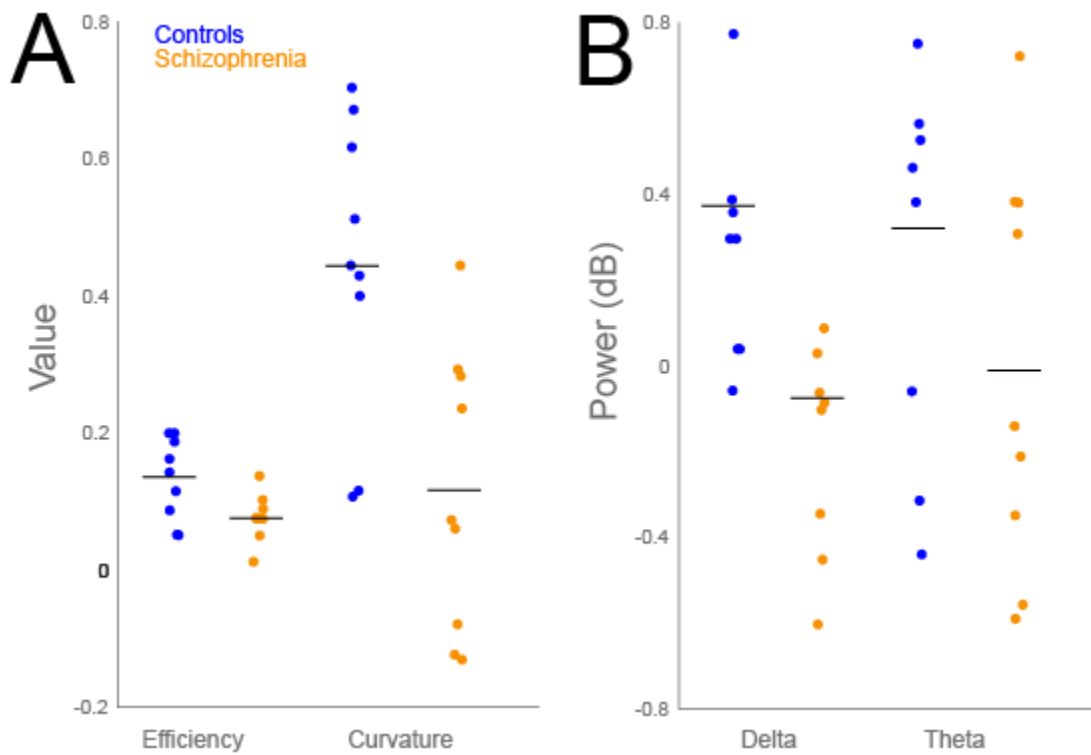
278 11 Kim J, Ghim J-W, Lee JH, Jung MW. Neural correlates of interval timing in rodent
279 prefrontal cortex. *J Neurosci Off J Soc Neurosci* 2013; **33**: 13834–13847.

280 12 Narayanan NS, Cavanagh JF, Frank MJ, Laubach M. Common medial frontal mechanisms of
281 adaptive control in humans and rodents. *Nat Neurosci* 2013; **16**: 1888–1897.

- 282 13 Rosenberg JR, Amjad AM, Breeze P, Brillinger DR, Halliday DM. The Fourier approach to
283 the identification of functional coupling between neuronal spike trains. *Prog Biophys Mol*
284 *Biol* 1989; **53**: 1–31.
- 285 14 Barnett L, Seth AK. The MVGC multivariate Granger causality toolbox: A new approach to
286 Granger-causal inference. *J Neurosci Methods* 2014; **223**: 50–68.
- 287 15 Cohen MX. *Analyzing Neural Time Series Data: Theory and Practice (Issues in Clinical and*
288 *Cognitive Neuropsychology)*. The MIT Press, 2014.
- 289

290

291 **Supplementary Figures**



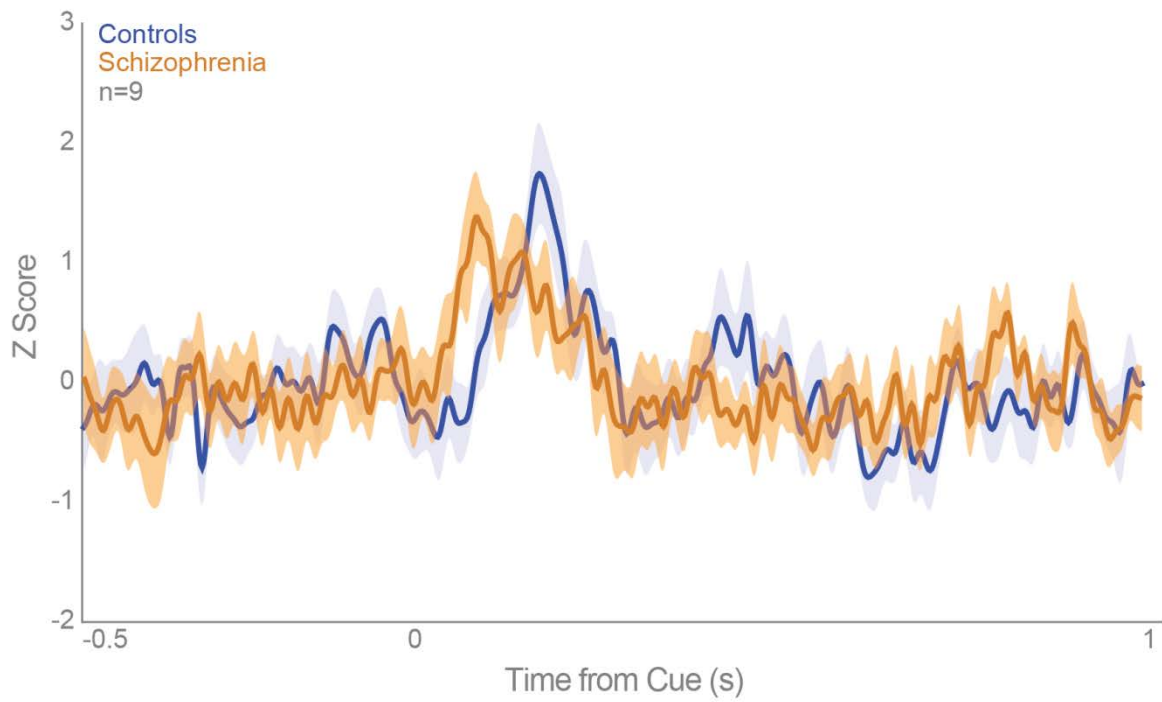
292

293 **Figure S1:** Individual subject data for Figure 1C (A) and Figure 1E (B). Each point is a single

294 subject for control (blue) and schizophrenic patients (orange).

295

296



297

298 **Figure S2:** Event-related potentials from patients with schizophrenia (orange) and

299 demographically-matched controls (blue).

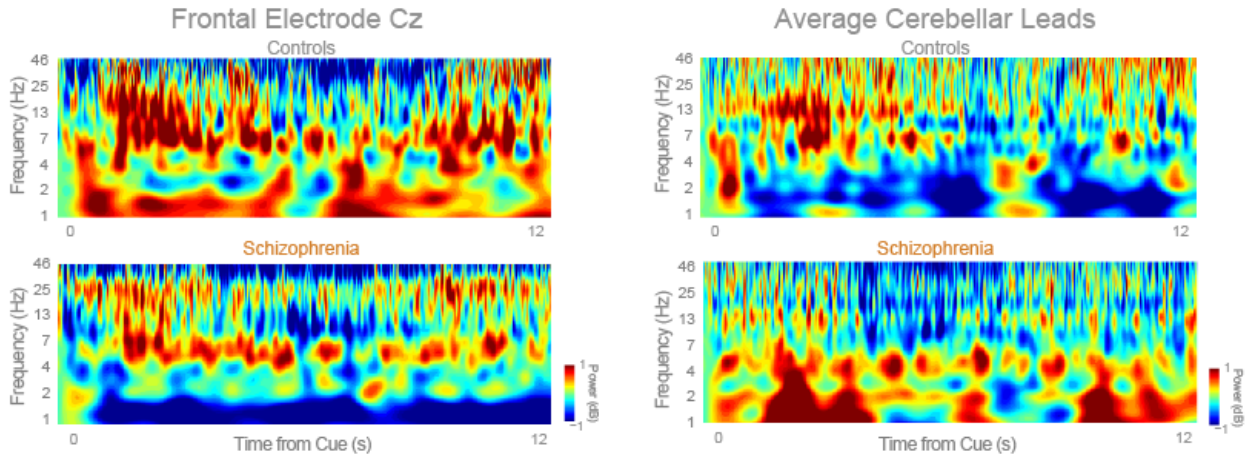
300

301

302

303

304



305

306 **Figure S3:** Time-frequency spectral plots reveal that patients with schizophrenia have decreased
 307 activity in the MFC throughout the interval in the interval timing task in comparison to healthy
 308 controls. Patients with schizophrenia can have low-frequency cerebellar activation in the
 309 interval timing task (9 patients vs. 9 controls).

310

311

312

313

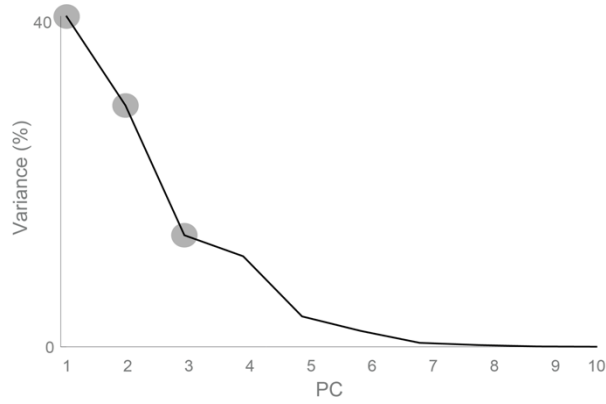
314

315

316

317

318



319

320 **Figure S4:** Scree plot of principal component analysis. Ramping activity was the most
321 prominent pattern of neural activity among both MFC and LCN neurons (PC1) explained ~40 %
322 of the variance.

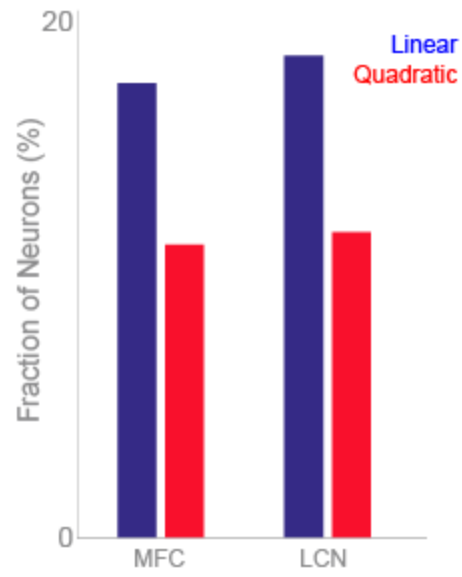
323

324

325

326

327



328

329 **Figure S5:** Number of MFC and LCN neurons with linear and quadratic coefficients via
330 regression. For MFC, 17% of neurons had a linear fit, and 11% had a quadratic fit; for LCN 18%
331 had a linear fit and 12% had a quadratic fit.

332

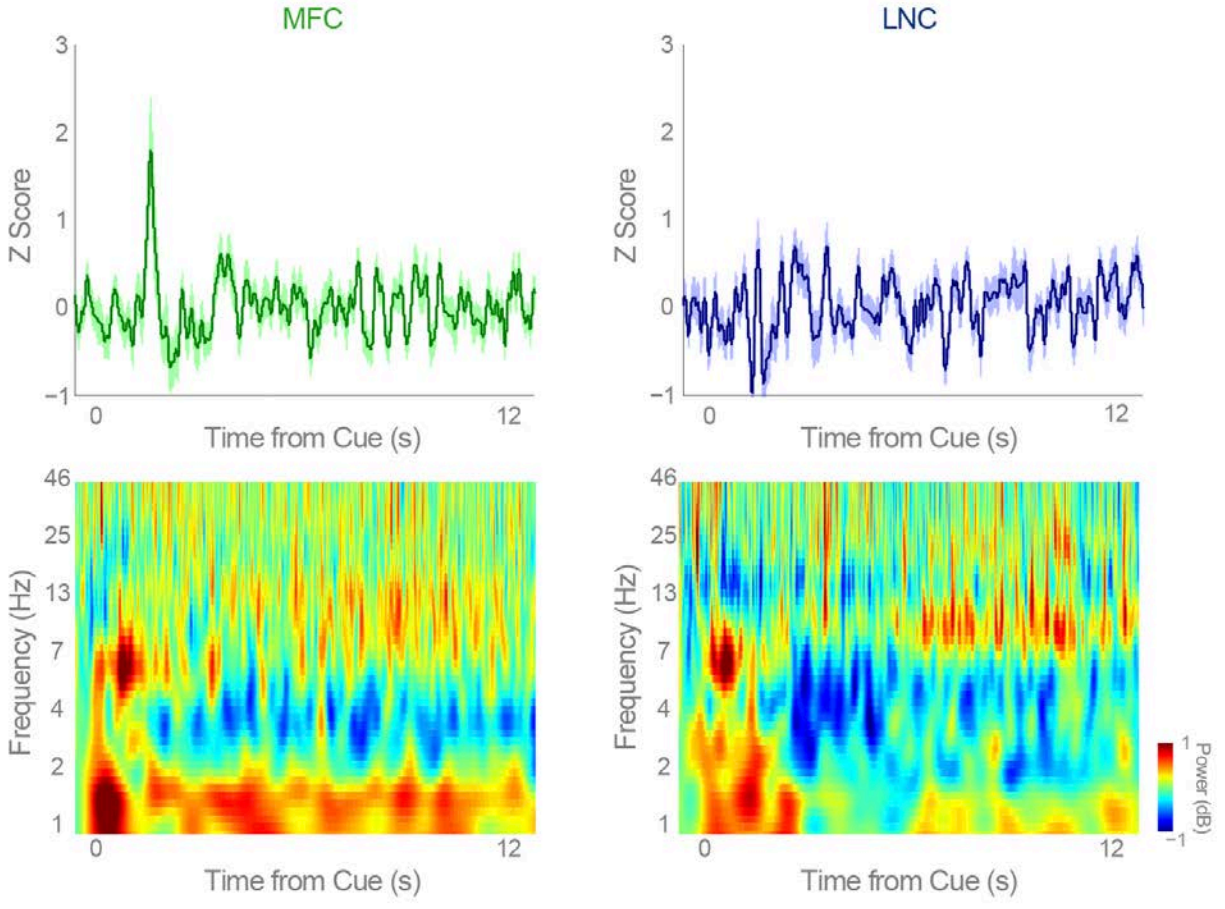
333

334

335

336

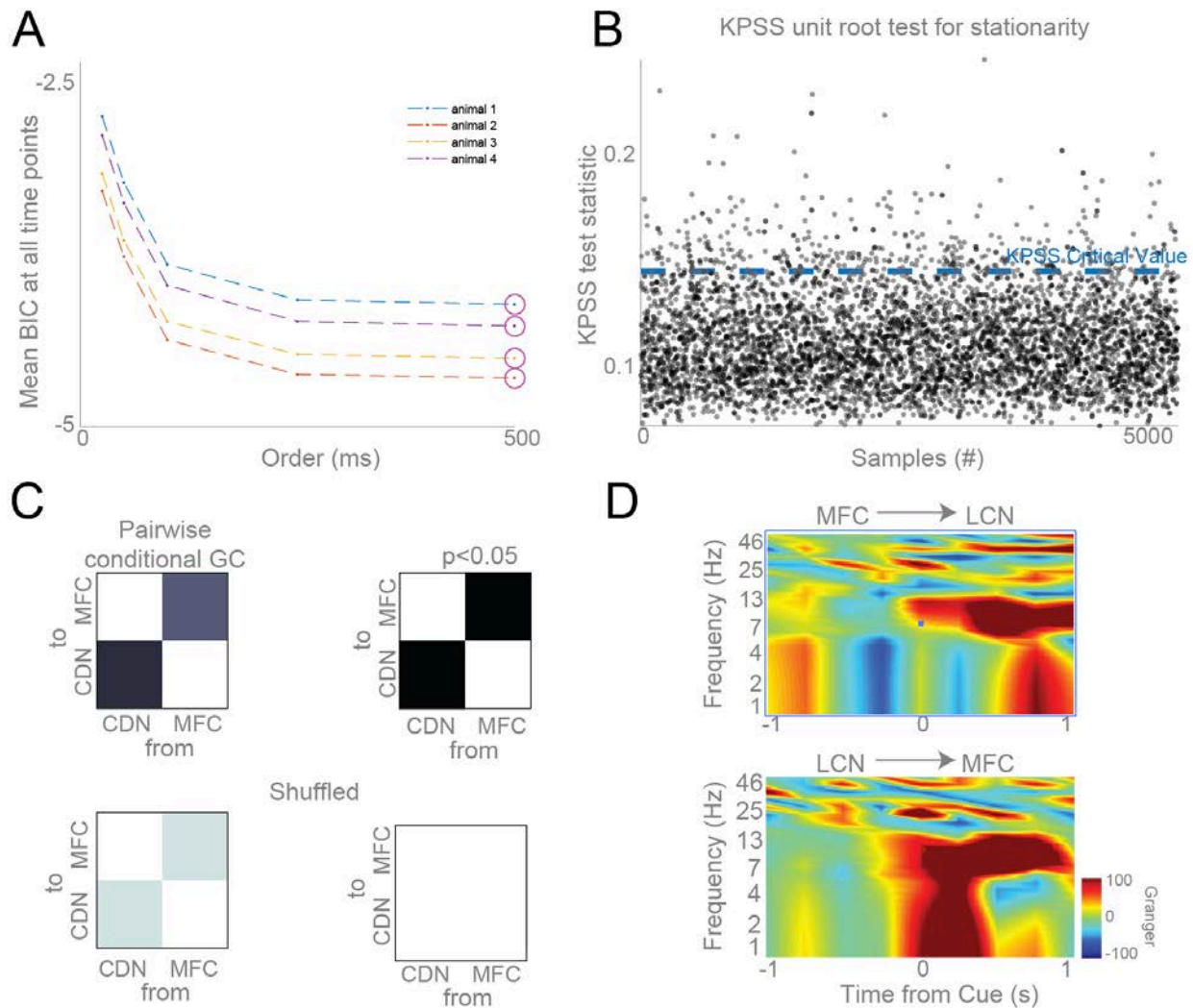
337



338

339 **Figure S6:** Field potentials and time-frequency plots of activity from the MFC and LCN.

340



341

342 **Figure S7:** Granger causality analyses. A) Mean Bayesian information criteria values across

343 segments converged to a stable minimum across orders > 100 ms, indicating minimized

344 regression error. We selected a model order of 500ms and 2000ms sliding time segments (6

345 segments per 12s interval timing trial) for subsequent analysis to maximize the resolution of low

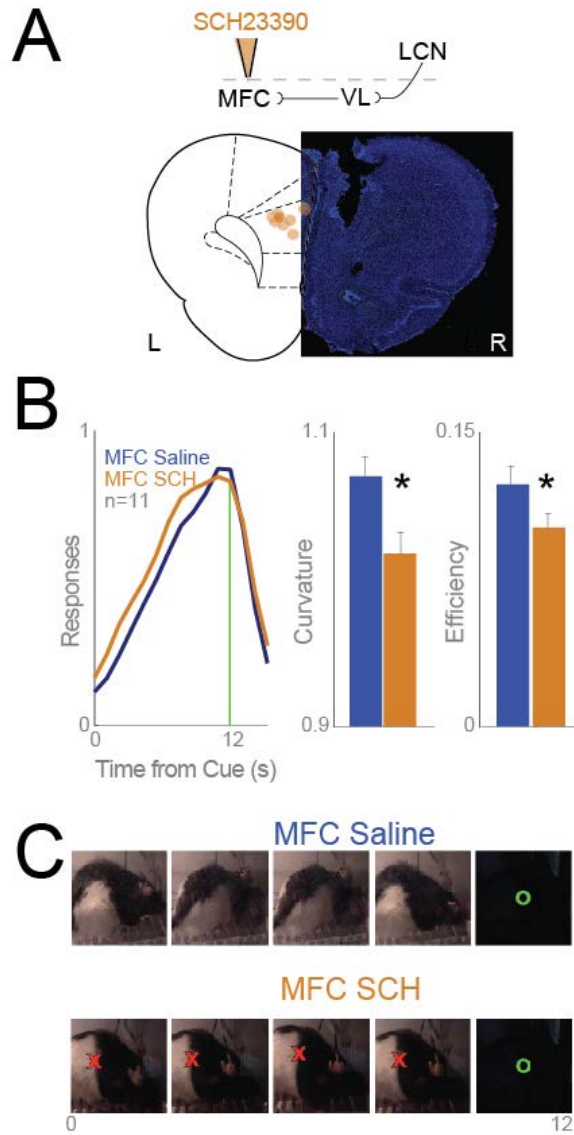
346 frequency Granger prediction. B) Corrected time series segments were submitted to KPSS unit

347 root testing using MVGC Toolbox routines to determine single trial KPSS test statistics to

348 determine stationarity. C) Significant Granger causality during 12s interval timing was assessed

349 using Granger's F-test routines in MVGC Toolbox at $p = 0.05$. Inputs were F-statistics averaged

350 across animals and time segments for directed connectivity between MFC and LCN in
351 experimental and time-shuffled data. D) Spectral pairwise Granger prediction indicates that the
352 cerebellar activity is predictive of activity in the medial frontal cortex at the time of trial start
353 ^{14,15} .
354



355

356 **Figure S8:** A) We modeled aspects of frontal dysfunction in schizophrenia in rodents by

357 unilaterally infusing the D1DR antagonist SCH23390 (orange) into the left (L).

358 Locations for each animal are represented by light blue dots on lower schematic with a

359 representative brain section at right (blue is DAPI). B) Rodents with unilateral MFC

360 SCH23390 infusions (orange; n=11) had broader estimates of the 12 second interval

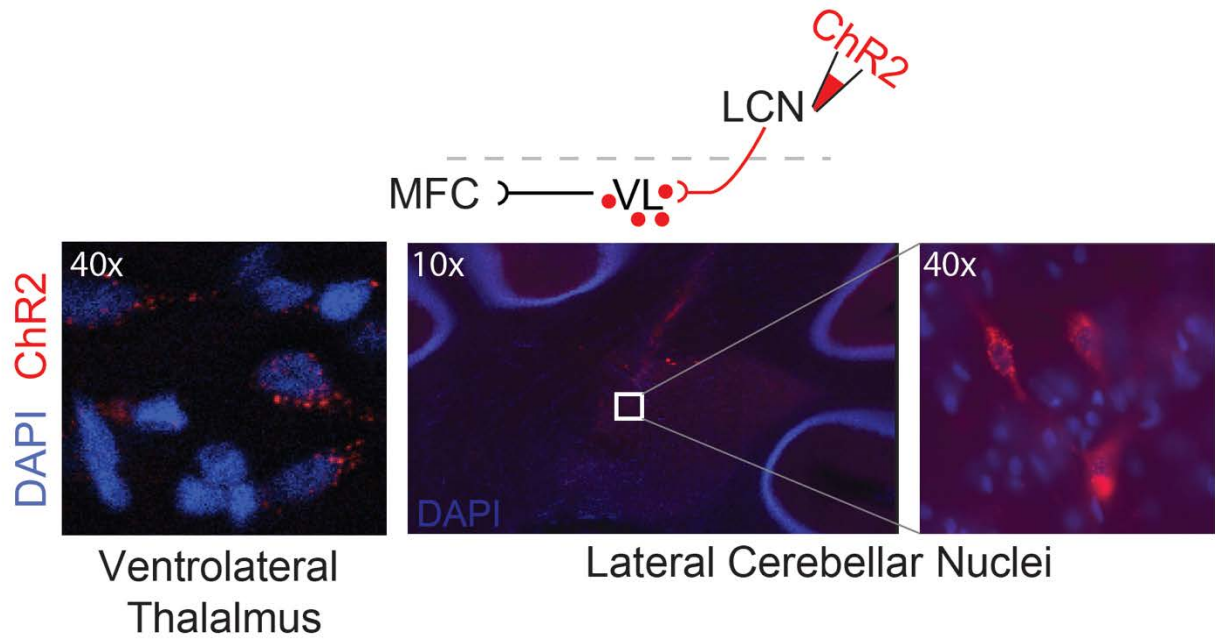
361 compared to control sessions, with saline infused into the MFC (blue). Time-response

362 histograms were flatter ($p < 0.02$) and animals were less efficient ($p < 0.004$) during interval

363 timing with MFC SCH23390. C) MFC SCH23390 did not change other aspects of
364 interval timing performance such as lever pressing or reward acquisition.

365

366



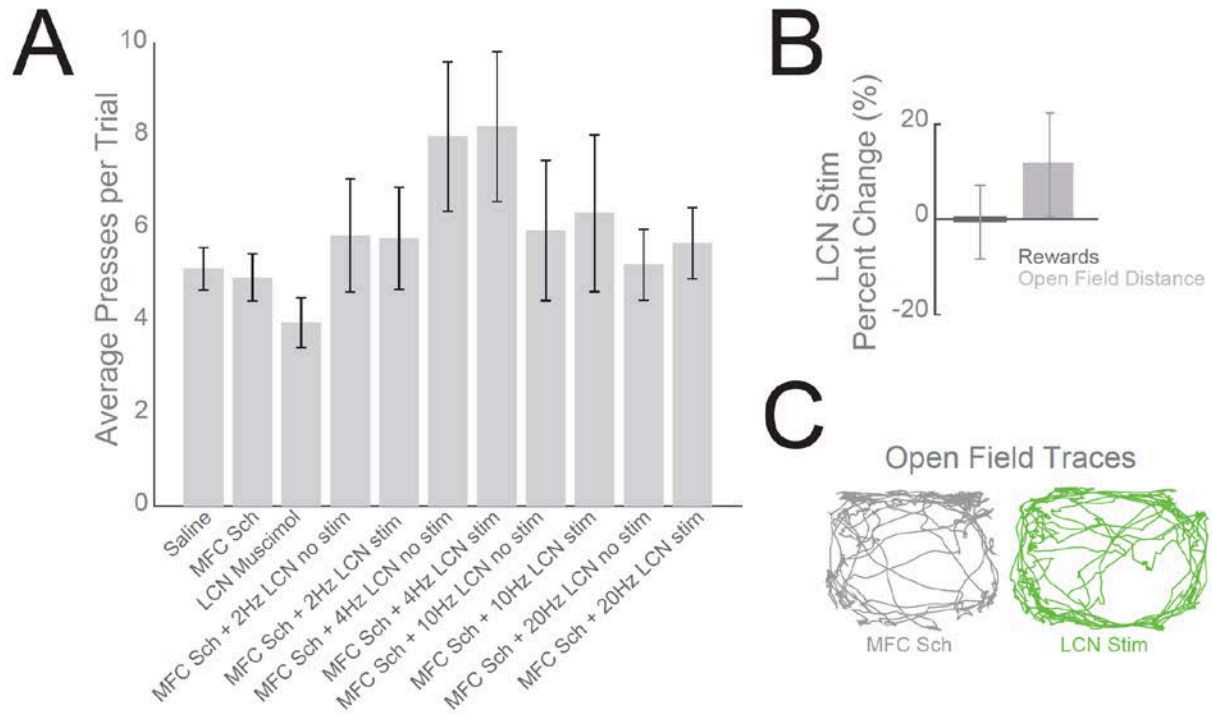
367

368

369

370 **Figure S9:** ChR2 infected cells at the injection site in the lateral cerebellar nuclei and in terminal

371 projections in the ventrolateral thalamus. Red is ChR2 and blue is DAPI.



372

373 **Figure S10:** There were no clear motor effects of LCN stimulation on A) the number of presses

374 per trial, B) rewards, or distance traveled in an open field. C) An example of open field distance

375 traveled in an animal with MFC D1 dopamine blockade without (gray) and with cerebellar

376 stimulation (green).

377

378

379

380

381

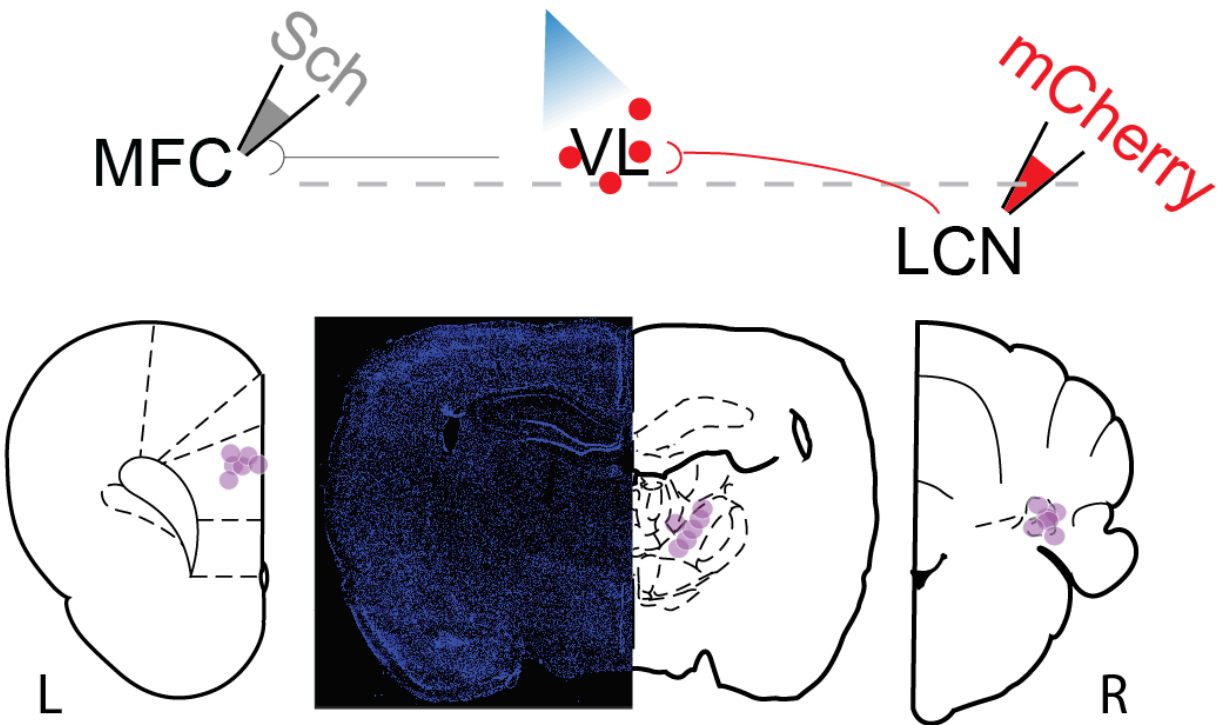
382

383

384

385

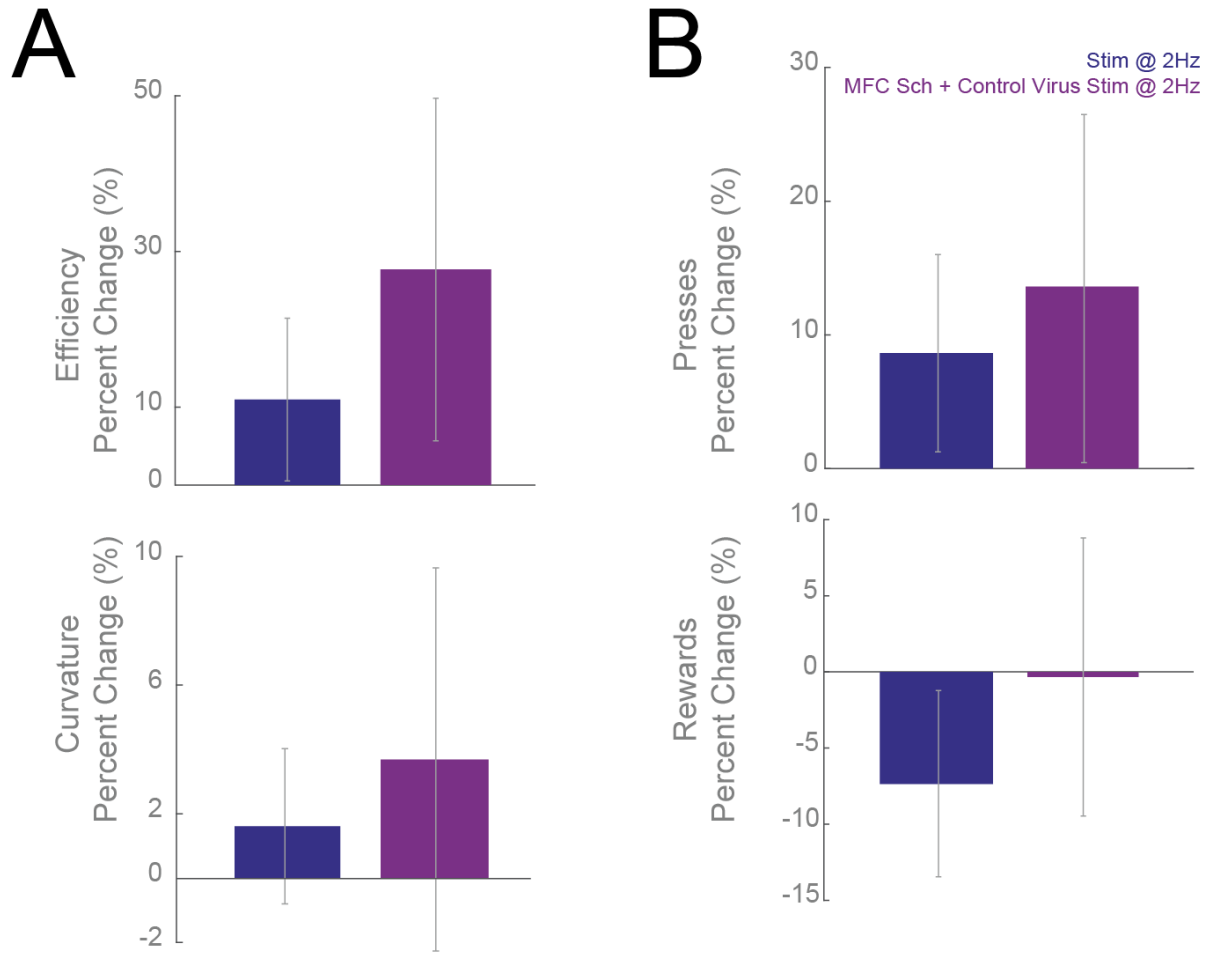
386
387
388
389
390
391



392
393
394
395
396
397
398
399

Figure S11: Optogenetic stimulation in 6 control animals did not significantly influence G) presses, H) rewards, I) interval timing efficiency, or J) curvature in time-response histograms.

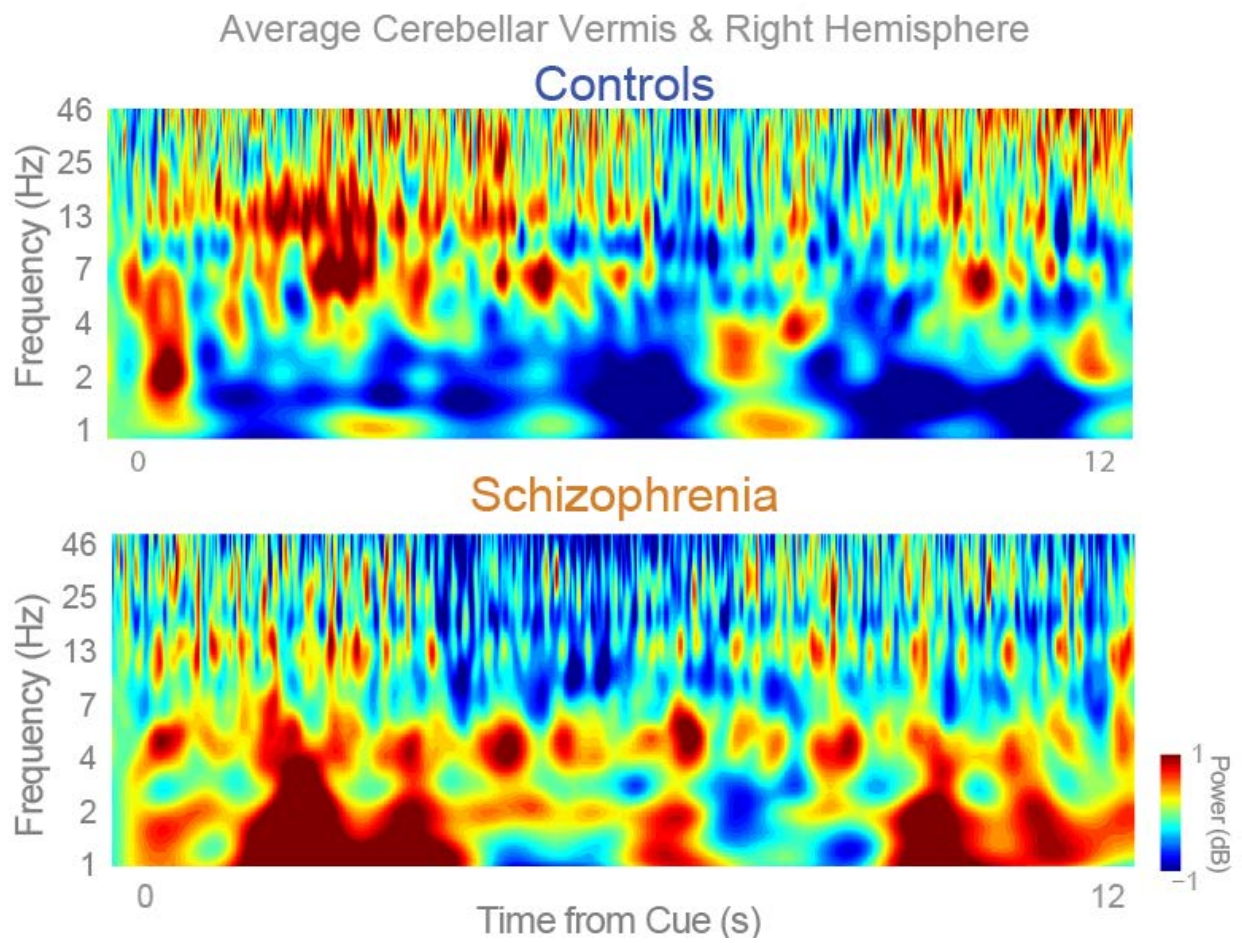
400
401
402
403



404
405
406
407
408
409
410

Figure S12: Optogenetic stimulation in 6 control animals did not significantly influence interval timing efficiency, curvature in time-response histograms, presses, or rewards.

411
412
413
414
415
416



417
418
419

Figure S13: Human EEG activity from cerebellar leads

420 **Supplementary Videos**

421

422 **Video S1:** A video of rodent with saline infused in MFC – most lever presses in these conditions
423 are towards the end of the interval.

424

425 **Video S2:** A video of the same rodent in Video S1 with the D1 antagonist SCH23390 infused
426 into the MFC. This animal had a disruption in behavior with many irrelevant responses. See
427 Narayanan et al., 2012; Parker et al., 2013; 2014, and 2015 for more details on this behavior.

428

429 **Video S3:** A video of the same rodent and on the same day on Video S2 on a LCN-VL 2 Hz
430 stimulation trial. This animal appeared to have fewer irrelevant responses and make more
431 responses towards the end of the interval.